# Coarse-graining the Self-assembly of $\beta$-helical Protein Building Blocks

**David Curcó,*,† Ruth Nussinov,‡,§ and Carlos Alemán*,||**

*Departament d'Enginyeria Química, Facultat de Química, Universitat de Barcelona, Martí i Franquès 1, Barcelona E-08028, Spain, Basic Research Program, SAIC-Frederick, Inc. Center for Cancer Research Nanobiology Program, NCI, Frederick, Maryland 21702, Department of Human Genetics Sackler, Medical School, Tel Aviv University, Tel Aviv 69978, Israel, and Departament d'Enginyeria Química, E. T. S. d'Enginyeria Industrial de Barcelona, Universitat Politècnica de Catalunya, Diagonal 647, Barcelona E-08028, Spain*

*Received: July 10, 2007; In Final Form: October 10, 2007*

Nanotubular structures constructed using self-assembled $\beta$-helical protein building blocks one atop the other have been coarsened to develop a mesoscopic potential that reproduces the intermolecular interaction energies provided by atomistic force-fields. The resulting potential consists of an analytical expression that depends exclusively on the distance and the relative orientation between the two interacting entities. In spite of its complexity, this coarse-grained potential reproduces satisfactorily the energetic properties of two interacting building blocks. The coarse-grained potential has been used to predict that the interaction between building blocks formed by residues 131−165 of *E. coli* galactoside acteyltransferase becomes repulsive when the size of the nanotube is larger than a threshold, that is, about 45 self-assembled building blocks.

## Introduction

The development of novel algorithms and the revolutionary advances in computer hardware technology that took place during the last two decades have allowed computer simulations of complex biological systems contributing to advance biomedical applications.[1−5] Computer simulations provide a unique tool to analyze the properties of large biomacromolecules with a level of detail difficult to obtain in other techniques. The excellent agreement between atomistic classical molecular dynamics (MD) simulation studies on conventional systems and experiments has permitted applications to assembled systems with increasing complexity. The latter studies have provided invaluable information about the nature of interactions such as protein−protein,[6,7] DNA−protein,[8] protein−lipid,[9,10] and DNA−lipid.[11]

In recent years, we have been focused on the construction of nanostructures using naturally occurring building blocks.[12−14] In particular, we are interested in assemblies comprised of protein fragments which constitute structural units that retain a conformation similar to the one they have when embedded in their corresponding native protein structures.[15−18] Within this context, we recently constructed stable nanotubular structures from monomeric naturally occurring $\beta$-helical building blocks.[17,18] For this purpose, building blocks were selected from native left-handed $\beta$-helical proteins by slicing $\beta$-helices into two-turn repeat units. Copies of each structural unit were stacked one atop the other, with no covalent linkage between them, using computer simulation methods. The stability of these self-assembled tube organizations was investigated through short (20−40 ns) atomistic MD simulations. Constructs able to preserve their organization in the simulation are candidates for experiments. We observed that a structural model based on the self-assembly of a two-turn repeat motif from *E. coli* galactoside acetyltransferase (PDB code 1krr, chain A) produced a very stable nanotube (Figure 1).[17] Next, the thermodynamical stability of this nanoconstruct was enhanced by introducing synthetic amino acids with conformational tendencies restrained to those of natural amino acids in the most mobile loop regions of the $\beta$-helical repeat sequence.[18,19]

Although the computational power is continuously increasing, the huge number of degrees of freedom involved at the atomistic level in these nanotubular structures limits the application of conventional MD approaches to study phenomena at the mesoscopic scale, that is, extended length and/or time scales. For instance, although structural phenomena on the ∼100 Å and ∼1 $\mu$s scales are of interest, conventional MD atomistic simulations of tubular nanostructures consisting of several tens of stacked $\beta$-helical building blocks are currently impossible since treating the atom−pair nonbonding interactions associated with such systems is unfeasible. Thus, only very short time and length scales can be currently reached in simulations of atomistic models owing to limitations of computer power, precluding investigation of some structural properties (for example, the persistence length and stiffness) and phenomena (for example, the diffusion of small molecules inside the tube and the application of nanotubes as drug delivery systems, etc) of the nanoconstruct. Therefore, new methodological improvements that permit an expansion of the time and length scales need to be developed.

One way to circumvent these problems is to reduce the degrees of freedom by a partial or even complete coarsening of the models, retaining only the degrees of freedom that are deemed important for a particular goal and target. Coarse-graining aims to guarantee that the global conformational relaxation, which takes orders of magnitude more in time than any local move, is achieved. This means that the characteristic

* Corresponding author. E-mail: curco@angel.qui.ub.es (D.C.) and carlos.aleman@upc.es (C.A.).
† Universitat de Barcelona.
‡ SAIC-Frederick, Inc. Center for Cancer Research Nanobiology Program.
§ Tel Aviv University
|| Universitat Politècnica de Catalunya.

10.1021/jp075386f CCC: $37.00 
Published on Web 11/21/2007

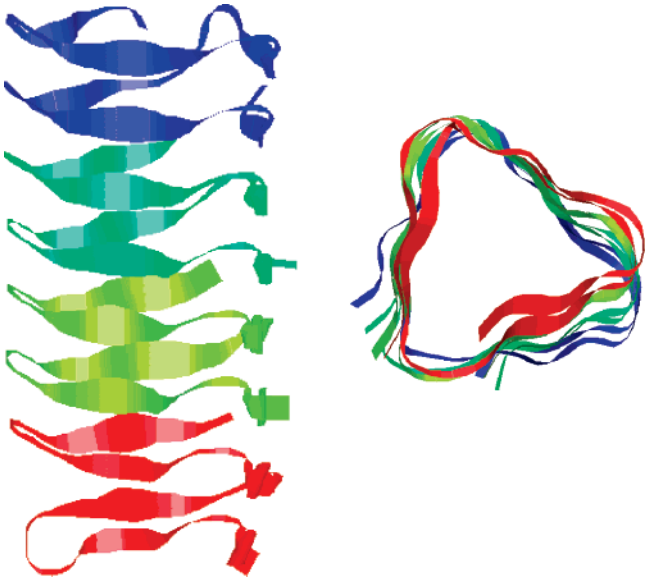

**Figure 1.** Axial (left) and equatorial (right) projection of the self-assembled nanotubular organization constructed using protein building blocks extracted from *E. coli* galactoside acetyltransferase (PDB code 1krr, chain A). Each building block is represented by a different color.

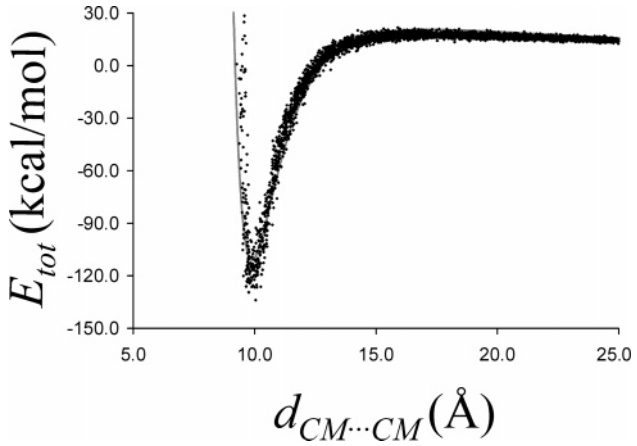


**Figure 2.** Graphical representation of the atomistic total interaction energy ($E_{tot}$) against $d_{cm-cm}$ for two interacting building blocks, where $E_{tot}$ is calculated using the AMBER force-field and $d_{cm-cm}$ is the distance between the center of masses of the building blocks. Continuous gray line corresponds to the total interaction energy calculated by summing the coarse-grained energies provided by eqs 1 and 2 (see text).

time step in MD simulation increases significantly; that is, fast degrees of freedom are eliminated, and the short spatial length scale is up-scaled. In a coarse-graining approach, the detailed chemistry enters only in the derivation of the potential between new interacting entities. The aim of the present work is within such context: in this study, we show that all nonbonding interactions between pairs of atoms belonging to two different building blocks of the tubular nanostructures can be coarse-grained to a single interaction between two mesoscopic entities, the building blocks.

Here, we report a simple coarse-grained model for the tubular nanostructures formed by self-assembled protein building blocks. For this purpose, we used atomistic configurations generated by classical MD of the tube formed by four stacked 1krr building blocks. However, this strategy can be applied to the nanostructures constructed using building blocks extracted from other proteins. In the proposed model, each building block is represented as a single particle; that is, it is a soft-physical model

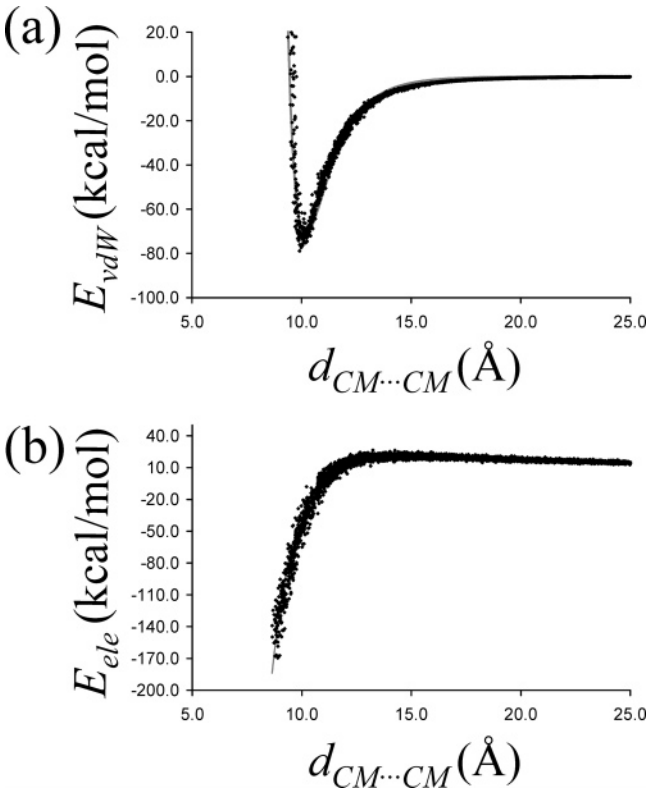


**Figure 3.** Graphical representation of the atomistic van der Waals (a) and electrostatic (b) interaction energy ($E_{vdW}$ and $E_{ele}$, respectively) against $d_{cm-cm}$ for two interacting building blocks, where the two energy contributions are calculated using the AMBER force-field and $d_{cm-cm}$ is the distance between the center of masses of the building blocks. Continuous gray lines correspond to the van der Waals (a) and electrostatic (b) energies calculated using the coarse-grained potentials displayed in eqs 1 and 2, respectively.

without any chemical information. Results have been used to examine the change in the stability of the nanotube with the number of self-assembled building blocks. We expect that this potential will further assist in multi-scale simulations of nanotubular structures in which a given part of the system (one/two building block/s) will be represented at the atomistic level while the rest of the system is described at the mesoscopic level. We plan on developing and testing this strategy in the near future.

## Computational Methods

MD simulations were performed using the NAMD program.[20] The simulated system consisted on four replicas of the left-handed β-helix formed by residues 131−165 of 1krr stacked one atop the other, with no covalent linkage between them, forming a tube. Table 1 describes the sequence of the 1krr building block. This system was placed in the center of an orthorhombic simulation box filled with explicit water molecules, which were represented using the TIP3 model.[21] Positively charged sodium atoms were added to the simulation box in the required amount to reach electrostatic neutrality. All atoms of the nanotube were considered explicitly, the total number of particles within the simulation box being 56238.

The energy was calculated by using the AMBER force-field,[22] the required parameters being taken from the AMBER libraries (parm95). Atom pair distance cutoffs were applied at 14 Å to compute van der Waals interactions. The electrostatic interactions were computed using the nontruncated electrostatic potential by means of Ewald summations.[23] The real space term

**TABLE 1: Sequence of the 1krr Building Block Used to Construct the Nanotube**

| PDB | protein name | residues | sequence |
|---|---|---|---|
| 1krr | galactoside acetyltransferase from *E. coli* | 131−165 | PITIGNNVWIGSHVVINP GVTIGDNSVIGAGSIVT |

was determined by the van der Waals cut off (14 Å), while the reciprocal term was estimated by interpolation of the effective charge into a charges mesh with a grid thickness of 5 points per volume unit, that is, particle−mesh Ewald (PME) method.[23] Bond lengths were constrained using the SHAKE algorithm,[24] the numerical integration step being 2 fs.

Before production simulations, the thermodynamic variables of the system were equilibrated. The energy of each system was initially minimized to relax conformational and structural tensions using the conjugate gradient method for $5 \times 10^3$ steps. After this, different consecutive rounds of short MD runs were performed in order to equilibrate the density, temperature, and pressure. First, solvent and charged sodium atoms were thermally relaxed by three consecutives runs, whereas the protein parts were kept frozen. 0.5 ns of NVT−MD at 500 K were used to homogeneously distribute the solvent and ions in the box. Next, 0.5 ns of isothermal and 0.5 ns isobaric relaxation were run. Finally, all of the atoms of the system were submitted to 0.15 ns of steady heating until the target temperature was reached (298 K), 0.25 ns of NVT-MD at 298 K (thermal equilibration) followed by 0.5 ns of density relaxation (NPT-MD). Both temperature and pressure were controlled by the weak coupling method, the Berendsen thermo-barostat,[25] using a time constant for heat bath coupling and a pressure relaxation time of 1 ps. The coordinates of the NPT-MD production run, which was 30 ns long, were saved every 10 ps intervals.

## Results and Discussions

**Stability of the Simulated Nanotube.** The stability of the nanotube derived from the self-assembly of the 1krr building block was extensively addressed and discussed in previous works.[17,18] The only difference between the simulations reported in those studies and those reported in the present one corresponds to the force-field. Previous simulations were performed with the CHARMM force-field,[17,18] while the present work has been carried out with AMBER force-field. As expected, results obtained with the two force-fields are in excellent agreement indicating that the stability predicted for the tubular nanoconstruct does not depend strongly on the choice of the force-field. As no new feature has been detected from the simulations with AMBER with respect to those published previously, detailed analyses of the stored microstructures to show the stability of the nanotube have been omitted in this article.

**Coarse-Graining the Interaction between Two Self-Assembled Building Blocks.** The goal of the present work is to develop a simple coarse-grained model able to describe the interaction between the $\beta$-helical building blocks found in self-assembled nanotubular structures. For this purpose, each building block has been represented as a single particle located at a physically reliable position, its center of mass. It is worth noting that solvent effects have been neglected for the development of such model. Indeed, solvent contributions are expected to play a crucial role in the self-assembly process, which is out of the scope of this work, but not on the stability of self-assembled nanotubes. Accordingly, explicit solvent molecules have been only used to obtain equilibrated and relaxed atomistic configurations of the building blocks. On the other hand, we focused on the reproduction of interactions energies, entropic effects being neglected because of the same reasons exposed above: (i) our coarse-grained model is a very physical (soft-)model without chemical information, and therefore, we can only reproduce simple properties at this level; and (ii) the model has not developed to study the self-assembly process by itself.

Initially, we investigated the variation of the atomistic intermolecular interaction energy between the two building blocks ($E_{tot}$) against the distance between the centers of masses ($d_{cm-cm}$) of two self-assembled building blocks. $E_{tot}$ was calculated as the sum of the electrostatic ($E_{ele}$) and van der Waals contributions ($E_{vdW}$), which are represented by the typical Coulombic and 12−6 Lennard-Jones expressions, respectively, in the AMBER force-field. Equilibrated and relaxed atomistic configurations of the building block, which were stored during the MD simulation (see Methods section), were used to generate new configurations using a simple algorithm that changes $d_{cm-cm}$ by introducing random displacements of the building block along the helical axis of the nanotube. In this way, we sampled a wide range of $d_{cm-cm}$ values (from 9.2 to 110.0 Å) on a large number of configurations. It should be emphasized that, on the basis of our previous experience on this system, movements based on axial displacement and rotation around this axis correspond to those typically detected at the atomistic level in the dynamics of the nanoconstruct.[18−20] Thus, motion sideways nor rotation around the plane perpendicular to the axis has been considered in this work because they are detected very rarely in the dynamics of the self-assembled nanoconstruct; that is, they are precluded by unfavorable interactions between the side chains of amino acids located at different building blocks. Each configuration stored during the MD simulation, which involves six pairs of interacting building-blocks, provided a new configuration, the total number of interacting pairs being {[3000 stored configurations] + [3000 new configurations]} × [6 pairs per configuration] = 36 000.

Figure 2 shows the variation of $E_{tot}$ against $d_{cm-cm}$, while the shape of the $E_{ele}$ and $E_{vdW}$ profiles is displayed in Figure 3. In all three cases, the variation of the atomistic energy with $d_{cm-cm}$ follows the tendency ideally expected for interactions between two noncovalently linked entities. The minimum of $E_{tot}$ was located at around $d_{cm-cm} = 9.9$ Å (Figure 2), the sum of two nonbonding contributions growing very rapidly when $d_{cm-cm}$ becomes smaller than such value. Inspection of the van der Waals profile (Figure 3a) indicates that short-range interactions become repulsive when $d_{cm-cm}$ is smaller than ∼9.5 Å, converging to zero when $d_{cm-cm}$ is ∼22 Å. On the other hand, the electrostatic profile (Figure 3b) shows that long-range interactions are attractive when $d_{cm-cm}$ is smaller than ∼11.3 Å but become repulsive for higher values, $E_{ele}$ growing with $d_{cm-cm}$ until ∼14.5 Å. This behavior, which is intimately related with the sequence of the building block, should be attributed to the unfavorable interaction between polar and/or ionized residues with similar distributions of atomic charges. After the latter value, a very slow convergence toward zero is detected. The repulsive character of the electrostatic interactions when $d_{cm-cm}$ is greater than ∼11.3 Å may have dramatic consequences on the stability of tubular nanostructures formed by a very large number of self-assembled building blocks. This topic will be specifically discussed below.

The atomistic contributions displayed in Figure 3 were adjusted to analytical expressions able to describe the van der Waals and electrostatic interactions between building blocks at the coarse-grained level:

$$V_{vdw} = \frac{2137.8}{d_{cm-cm}^{16}} - \frac{2826.3}{d_{cm-cm}^{11}} \quad (1)$$

$$V_{ele} = -\frac{840}{d_{cm-cm}^{-6.84}} + \frac{1081}{d_{cm-cm}} + \frac{11697}{d_{cm-cm}^{2}} \quad (2)$$

The quality of the adjustments is excellent in both cases as evidenced by (i) atomistic energies which perfectly match the profiles derived from such coarse-grained potentials (included in Figure 3) and (ii) the statistical parameters of the fittings, that is, correlation coefficients greater than 0.98 and root-mean-square deviations lower than 3.4 kcal/mol. Unfortunately, the potentials displayed in eqs 1 and 2 are only valid when the relative orientation between the interacting building blocks is fixed at the optimum value provided by the atomistic MD simulation. Thus, although atomistic MD simulations indicated that this kind of movement is relatively unfrequent, it cannot be considered as rare. In order to obtain coarse-grained potentials able to describe interactions in the whole potential energy hypersurface, the influence of the relative orientation between the interacting building blocks on the atomistic energies must also be sampled.

The interaction energy is expected to depend on the relative orientation of the two building blocks, this feature being especially evident for short distances. Pilot calculations indicated that the stability of the self-assembled nanoconstruct depends on how efficient is the match between consecutive building blocks. Homogeneous β-helix folds can be obtained by forming stable assemblies of building blocks aligned in a complementary (self-assembled) manner. Accordingly, small variations in the relative orientation of two elements separated by a short distance produce severe repulsive interactions.

The dihedral angle ($\phi$) defined by the geometric center of the atoms contained in VAL(138) of the first building block, the center of masses of the two building blocks, and the geometric center of the atoms contained in VAL(157) of the second building block was used to define the relative orientation between two interacting entities. It should be noted that the choice of the two VAL residues used to define the end points of $\phi$ is completely arbitrary. Indeed, we checked that the strategy defined along this work to model the self-assembled nanoconstruct can be reproduced choosing different residues; that is, the only restriction is that the selected residues must belong to different building blocks.

The influence of the orientation on the atomistic energies was sampled systematically by considering different $d_{cm-cm}$ values for each $\phi$. In order to illustrate the results, Figure 4 shows the $E_{tot}$ profiles obtained for selected values of $\phi$. As can be seen, the shape of such profiles is very similar in all cases, even though $\phi$ has a significant influence on the strength of the interaction at the $d_{cm-cm}$ value of the lowest energy. The analytical expression that provided the best fitting to the total atomistic energies of the 4426 generated structures was:

$$V_{tot} = k_0 + \left\{ \begin{array}{l} k_1 \dfrac{\phi(2\pi-\phi)^{0.5}}{d_{cm-cm}^{16}} + \dfrac{k_2}{d_{cm-cm}^{16}} + \dfrac{k_3}{d_{cm-cm}^{11}} + k_4 \dfrac{\cos 3\phi}{d_{cm-cm} - 6.48} + \\ k_5 \dfrac{\phi(2\pi-\phi)^{0.5}}{d_{cm-cm}{}^{2}} + k_6 \dfrac{\sin 3\phi[\phi(2\pi-\phi)^{0.5}]}{d_{cm-cm}} + \\ k_7 \exp[-0.01(30 - d_{cm-cm}{}^{2})] + k_8 \dfrac{\cos 3\phi}{d_{cm-cm}{}^{3}} \end{array} \right\} \sigma(d_{cm-cm}) \quad (3)$$

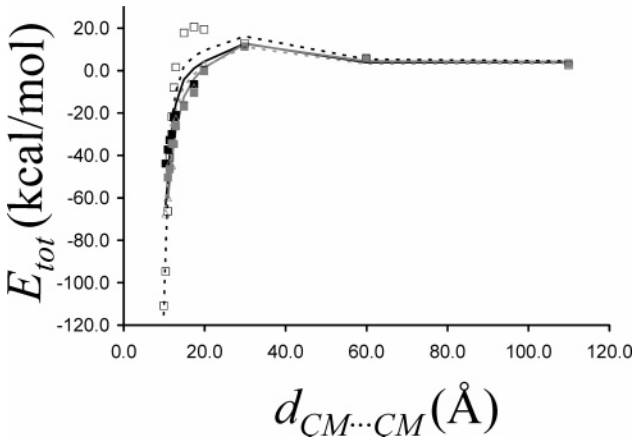


**Figure 4.** Graphical representation of the atomistic total (symbols) and coarse-grained (lines) interaction energy ($E_{tot}$) against $d_{cm-cm}$ for two interacting building blocks that are arranged forming a dihedral angle $\phi$ of 0° (empty squares and black dashed line), 2° (empty triangles and gray dashed line), 5° (filled squares and gray line) and 15° (filled triangles and black line). Coarse-grained energies have been calculated using the potential displayed in eq 3.

**TABLE 2: Constants ($k_i$ with $i$ Ranging from 0 to 8 in eq 3) for the Coarse-Grained Potential Obtained for the Self-Assembly of the 1krr Building Blocks**

| | | |
|---|---|---|
| $k_0 = 3.56$ | $k_3 = -2 \times 10^{13}$ | $k_6 = -2446.6$ |
| $k_1 = 3 \times 10^{17}$ | $k_4 = 106.49$ | $k_7 = 9.64$ |
| $k_2 = 1 \times 10^{18}$ | $k_5 = -1084.4$ | $k_8 = -42228$ |

where $k_i$ with $i$ ranging from 0 to 8 are the constants listed in Table 2 and $\sigma(d_{cm-cm})$ is a sigmoidal function that depends on $d_{cm-cm}$,

$$\sigma(d_{cm-cm}) = \frac{1 - \exp(-10 d_{cm-cm})}{1 + \exp(-10 d_{cm-cm})} \quad (4)$$

The correlation coefficient and the root-mean-square deviation of the fitting that led to eq 3 was 0.95 and 3.77 kcal/mol, respectively. Although the range of validity of eqs 3 and 4 in terms of $\phi$ is 360°, the description of the atomistic model was worse for the regions associated to very repulsive interaction energies ($\phi = 0°$ in Figure 4) because of statistical reasons; that is, the statistical description of high repulsive values, which are the less frequent, was poor in the fitting.

The potential obtained when both $d_{cm-cm}$ and $\phi$ are considered in the adjustment is significantly more complex than those displayed in eqs 1 and 2. Similarly, complex potentials are also provided when the electrostatic and van der Waals contributions are considered separately, with no advantage being obtained in this case from such separation. While computationally the potential displayed in eq 3 appears complex and more demanding than simple atomistic potentials, it is nevertheless very practical: it allows rapid evaluation (in a single step) of the total interaction energy between two building blocks, saving the computational time and memory which are required for the calculations with atomistic nonbonding pair potentials. For the 1krr building block, which consists of 493 explicit atoms, the evaluation of the van der Waals and electrostatic interaction energies at the atomistic level involves the calculation of $2 \times (493 \times 493) = 486\,098$ pair potentials.

The objective of coarse-grained models is to reduce the number of degrees of freedom characteristic of atomistic models to investigate phenomena at the mesoscopic scale. In the coarse-graining approach, the detailed chemistry enters only in the derivation of the potential between new interacting entities.

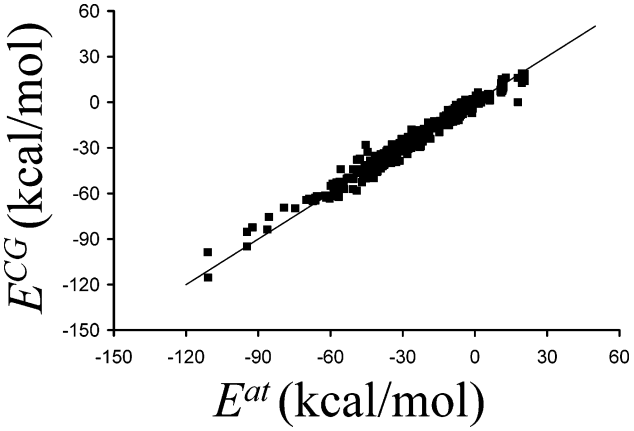


**Figure 5.** Graphical representation of the atomistic total energies ($E^{at}$) vs the coarse-grained total energies ($E^{CG}$) for 500 independent configurations, which have not been used in the development of the coarse-grained potential.

Therefore, the chemical meaning of atomistic potentials is completely absent in coarse-graining potentials, especially when the size of the interacting entities is very large. The potential displayed in eq 3 allows a significant expansion of time and length scales, even though the elimination of degrees of freedom characteristic of atomistic models led to an increase the complexity of the analytical expression and to elimination of its chemical rationalization.

The coarse-grained potential displayed in eq 3 may be used in multi-scale simulations, in which a part of the system (a reduced number of building blocks) is represented by atomistic classical force-fields and the rest is described using mesoscopic entities. This is a very promising field of research within nanotech since both microscopic chemical details and phenomena typically found in the mesoscopic metric are involved in the same simulation. We plan to address this type of simulation in the near future.

**Test Calculations.** The reliability of the potential model proposed in eq 3 has been tested by comparing the atomistic and coarse-grained total energies calculated for 500 independent configurations, which were obtained for this purpose. These structures were derived from 500 very short MD simulations (~5 ps) of a system consisting of two 1krr building blocks. In order to sample all of the configurational space, starting structures were generated assigning random values to $d_{cm-cm}$ and $\phi$. Thus, the role of the short MD simulations was only to relax the initial structures, especially when $d_{cm-cm}$ was shorter than 10 Å. Figure 5 compares the interaction energy between building blocks of such structures calculated using the atomistic model (AMBER force-field) and the coarse-grained model (potential displayed in eqs 3 and 4). As can be seen, there is an excellent agreement between the two methodologies, the correlation coefficient, scaling coefficient $c$ ($y = cx$), and root-mean-square deviation being 0.98, 0.97, and 4.1 kcal/mol, respectively. It should be noted that these statistical parameters are remarkably good, especially if we consider that the atomistic energies range from −111 to 21 kcal/mol. These results clearly demonstrate that the coarse-grained potential derived in this work to determine at the mesoscopic level the strength of the interaction between two building blocks is satisfactory. On the other hand, analyses of the computational resources required by both the atomistic model and this CG approach indicate that calculations with the latter are faster than with the former by about 2−3 orders of magnitude, depending on the performance of the CPU.

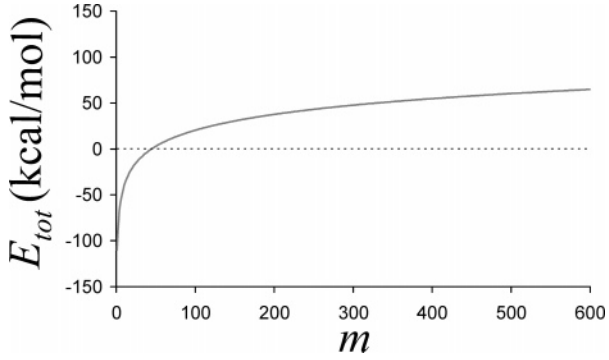


**Figure 6.** Variation of the total interaction energy ($E_{tot}$) with the number of 1krr building blocks contained in the nanotube ($m$).

**$\beta$-Helical Protein Nanotubes.** The potential displayed in eq 3 has been used to examine the stability of large nanotubes formed by self-assembled 1krr building blocks. Figure 6 represents the variation of the total interaction energy with the number of building blocks contained in the nanotube $m$, where $m$ ranges from 2 to 600. The interacting building blocks were arranged considering the lowest energy arrangement in terms of $d_{cm-cm}$ and $\phi$. As can be seen, the tubes formed by a small number of building blocks are very stable, even though the stability decreases very rapidly when $m$ increases. Thus, the nanotube becomes an unfavored supramolecular structure for $m > 45$. After this, the destabilization of the tubular nanoconstructs grows progressively but slowly. These results should be considered only from a qualitatively point of view because of the simple nature of our model. The shape of the profile displayed in Figure 6 must be attributed to the repulsive contribution when $d_{cm-cm}$ is higher than 12−20 Å, the exact value depending on $\phi$ (see Figure 4). Thus, the interaction energy between two consecutive building blocks (1−2 interactions) is always attractive, but the interaction with the next building blocks ($1 - n$ interactions with $n > 2$) is slightly repulsive or zero (when $n$ is very large). Accordingly, the favorable 1−2 interactions are predominant when $m$ is relatively small, but the repulsive term becomes the most important when the length of the nanotube is larger than a threshold.

It should be emphasized that the strategy presented in this work to simulate large nanotubes formed by self-assembled $\beta$-helices can be easily applied to other nanoconstructs. Specifically, recent studies on self-assembled amyloid systems indicated that the $\beta$-sheet growth and sheet−sheet packing can be controlled by modulating the concentration of metal ions in the medium.[26,27] The use of theoretical prediction on a large length-scale combined with experimental evidence on self-assembled architectures offers may allow the development of novel materials based on such scaffolds.

## Conclusions

This work reports a coarse-grained potential able to provide a very satisfactory representation of the stability of self-assembled nanotubular constructs made of $\beta$-helical protein building blocks. To derive the potential, each building block has been considered as a single entity, the relative arrangement between two interacting building blocks being described by a distance and a dihedral angle. Although the analytical expression of the coarse-grained potential is very complex, the total interaction energy is calculated in a single step. This represents a significant advance in terms of computer resources with respect to atomistic classical force-fields. The derived coarse-grained potential has been used to examine the variation of the stability

of the nanotube with the number of self-assembled building blocks. Results reveal that the interaction between the building blocks becomes repulsive after a threshold value.

It is worth noting that the reported coarse-grained model is not expected to be valid for the simulation of the self-assembly process because atomistic structures constituted by self-assembled elements were the only considered for its development. However, the results presented in this work are expected to be useful in future investigations in which multiscale simulations of large nanotubes, that is, about 30−40 self-assembled building blocks, will be performed combining atomistic and coarse-grained models. Thus, these simulations will allow prediction of the mesoscopic properties of the nanostructure but retain simultaneously the microscopic chemical details in a small selected region of the system.

**Acknowledgment.** The authors are indebted to the Barcelona Supercomputer Center (BSC) and to the Centre de Supercomputació de Catalunya (CESCA) for computational facilities. Dr. David Zanuy is thanked for his kind assistance in Molecular Dynamics simulations. This project has been funded in whole or in part with Federal funds from the National Cancer Institute, National Institutes of Health, under Contract No. N01-CO-12400. The content of this publication does not necessarily reflect the view of the policies of the Department of Health and Human Services, nor does mention of trade names, commercial products, or organization imply endorsement by the U.S. Government. This research was supported [in part] by the Intramural Research Program of the NIH, National Cancer Institute, Center for Cancer Research.

## References and Notes

(1) Sanbonmatsu, K. Y.; Tung, C. S. *J. Struct. Biol.* **2007**, *157*, 470.
(2) Shakhonoich, E. *Chem. Rev.* **2006**, *106*, 1559.
(3) Efremoy, R. G.; Nolde, D. E.; Konshina, A. G.; Syrtcev, N. P.; Arseniev, A. S. *Curr. Med. Chem.* **2004**, *11*, 2421.
(4) Saiz, K.; Klein, M. L. *Acc. Chem. Res.* **2002**, *35*, 482.
(5) Warsel, A. *Acc. Chem. Res.* **2002**, *35*, 385.
(6) Tsai, H.-H.; Tsai, C.-J.; Ma, B.; Nussinov, R. *Protein Sci.* **2004**, *13*, 2753.
(7) Orban, T.; Kalafatis, M.; Gogonea, V. *Biochemistry* **2005**, *44*, 13082.
(8) Villa, E.; Balaeff, A.; Schulten, K. *Proc. Natl. Acad. Sci.* **2005**, *102*, 6783−6788.
(9) Sansom, M. S. P.; Bond, P. J.; Deol, S. S.; Grottesj, A.; Haider, S.; Sands, Z. A. *Biochem. Soc. Trans.* **2005**, *33*, 916.
(10) Friedman, R.; Nachliel, E.; Gutman, M. *Biochemistry* **2005**, *44*, 4275−4283.
(11) Bandyopadhyaya, S.; Tarek, M.; Klein, M. L. *J. Phys. Chem. B* **1999**, *103*, 10075.
(12) Alemán, C.; Zanuy, D.; Jiménez, A. I.; Cativiela, C.; Haspel, N.; Zheng, J.; Wolfson, H.; Nussinov, R. *Phys. Biol.* **2006**, *3*, S54.
(13) Tsai, C.-J.; Zheng, J.; Alemán, C.; Nussinov, R. *Trends. Biotech.* **2006**, *24*, 449.
(14) Tsai, C.-J.; Zheng, J.; Zanuy, D.; Haspel, N.; Wolfson, H.; Alemán, C.; Nussinov, R. *Proteins* **2007**, *68*, 1.
(15) Tsai, H.-H.; Tsai, C.-J.; Ma, B.; Nussinov, R. *Protein Sci.* **2004**, *13*, 2753.
(16) Tsai, C.-J.; Zheng, J.; Nussinov, R. *PLoS Computational Biology* **2006**, *2*, e42.
(17) Haspel, N.; Zanuy, D.; Aleman, C.; Wolfson, H.; Nussinov, R. *Structure* **2006**, *14*, 1137.
(18) Zheng, J.; Zanuy, D.; Haspel, N.; Tsai, C.-J.; Alemán, C.; Nussinov, R. *Biochemistry* **2007**, *46*, 1205.
(19) Zanuy, D.; Jiménez, A. I.; Cativiela, C.; Nussinov, R.; Alemán, C. *J. Phys. Chem. B* **2007**, *111*, 3236.
(20) Kale, L.; Skeel, R.; Bhandarkar, M.; Brunner, R.; Gursoy, A.; Krawetz, N.; Phillips, J.; Shinozaki, A.; Varadarajan, K.; Schulten, K. *J. Comput. Phys.* **1999**, *151*, 283.
(21) Jorgensen, W. L.; Chandrasekhar, J.; Madura, J. D.; Impey, R. W.; Klein, M. L. *J. Chem. Phys.* **1983**, *79*, 926.
(22) Cornell, W. D.; Cieplak, P.; Bayly, C. I.; Gould, I. R.; Merz, K. M.; Ferguson, D. M.; Spellmeyer, D. C.; Fox, T.; Caldwell, J. W.; Kollman, P. A. *J. Am. Chem. Soc.* **1995**, *117*, 5179.
(23) Darden, T.; York, D.; Pedersen, L. *J. Chem. Phys.* **1993**, *98*, 10089.
(24) Ryckaert, J. P.; Ciccotti, G.; Berendsen. H. J. C. *J. Comput. Phys.* **1977**, *23*, 327.
(25) Berendsen, H. J. C.; Postma, J. P. M.; van Gunsteren, W. F.; DiNola, A.; Haak, J. R. *J. Chem. Phys.* **1984**, *81*, 3684.
(26) Dong, J.; Shokes, J. E.; Scott, R. A.; Lynn, D. G. *J. Am. Chem. Soc.* **2006**, *128*, 3540.
(27) Dong, J.; Canfield, J. M.; Mehta, A. K.; Shokes, J. E.; Tian, B.; Childers, W. S.; Simmons, J. A.; Mao, Z.; Scott, R. A.; Warncke, K.; Lynn, D. G. *Proc. Natl. Acad. Sci. U.S.A.* **2007**, *104*, 13313.